

Transformation of Epithelial Ovarian Cancer Stemlike Cells into Mesenchymal Lineage via EMT Results in Cellular Heterogeneity and Supports Tumor Engraftment

Hua Jiang,^{1,5*} Xiaolong Lin,^{1,5*} Yingtao Liu,^{1,5*} Wenjia Gong,¹ Xiaoling Ma,¹ Yinhua Yu,¹ Yi Xie,² Xiaoxi Sun,³ Youji Feng,¹ Viktor Janzen,⁴ and Tong Chen²

¹Department of Gynecology, Obstetrics and Gynecology Hospital, Fudan University, Shanghai, China; ²Department of Hematology, Huashan Hospital, Fudan University, Shanghai, China; ³Shanghai Jiai Genetics & IVF Institute, Shanghai, China; ⁴Department for Internal Medicine III, Hematology and Oncology, University-Hospital of Bonn, Bonn, Germany

Ovarian cancers are heterogeneous and contain stemlike cells that are able to self-renew and are responsible for sustained tumor growth. Metastasis in the peritoneal cavity occurs more frequently in ovarian cancer than in other malignancies, but the underlying mechanism remains largely unknown. We have identified that ovarian cancer stemlike cells (CSCs), which were defined as side population (SP) cells, were present in patients' ascitic fluid and mesenchymally transformed cell lines, ES-2 and HO-8910PM. SP cells, which were sorted from both cell lines and implanted into immunocompromised mice, were localized to the xenografted tumor boundary. In addition, SP cells exhibited an epithelial phenotype and showed a distinct gene expression profile with reduced expression of cell adhesion molecules (CAMs), indicating that SP cells exert an important role in ovarian cancer progression on the basis of their delicate interaction with the surrounding microenvironment and anatomical localization in tumors. In contrast, non-SP cells exhibited a more mesenchymal phenotype and showed more increased invasive potential than SP cells. This heterogeneity was observed as an endogenous transformation via the epithelial-mesenchymal transition (EMT) process. Inhibition of the EMT process by Snail1 silencing reduced the SP cell frequency, and affected their invasive capacity and engraftment. These findings illustrate the interplay between epithelial ovarian CSCs and the EMT, and exert a link to explain tumor heterogeneity and its necessity for ovarian cancer maintenance, metastasis and progression.

Online address: <http://www.molmed.org>

doi: 10.2119/molmed.2012.00075

INTRODUCTION

The question of whether tumor growth is driven by cancer stem cells (CSCs) has been discussed for decades (1–4). The elucidation of the molecular mechanisms that govern CSC function might advance our understanding of tumorigenesis and provide potential new targets for anti-cancer therapy. CSCs in solid tumors

have been identified by utilizing various surface marker combinations, including CD44⁺ and CD24⁻ (5), CD133⁺ (6), CD133⁺ and CXCR4⁺ (7), CD44⁺ and CD24⁺ (8), ATP-binding cassetteB5 (9), epithelial cell adhesion molecule (EpcAM; 10) and aldehyde dehydrogenase (ALDH) activity (11). Side population (SP) cells from various tumor tissues

which exhibit stemlike features have been isolated using the fluorescent DNA-binding dye Hoechst 33342 (12–14). However, CSC phenotype may not be uniform between cancer subtypes of the same organ or even tumors of the same histological subtype. Cellular and functional heterogeneity within the tumor cells may lead to different disease manifestations, variable response to cancer treatment and drug resistance of tumor cells (15).

Ovarian cancer is the most lethal gynecological malignancy. The majority of patients present at an advanced stage with widely metastatic sites within the peritoneal cavity, leading to high mortality (16). However, the mechanism for how ovarian cancer cells metastasize within the peritoneal cavity is not known.

There are several lines of evidence that the process of epithelial-mesenchy-

*HJ, XL and YL contributed equally to this paper.

Address correspondence to Tong Chen, Department of Hematology, Huashan Hospital, Fudan University, Shanghai 200040, China. Phone: +86-21-52889999; Fax: +86-21-62489191; E-mail: chentong@fudan.edu.cn; or Viktor Janzen, University Hospital Bonn, Bonn, Germany. Phone: +49-228287-51700; Fax: +49-228287-9080052; E-mail: viktor.janzen@ukb.uni-bonn.de; or Youji Feng, OB&GYN Hospital of Fudan University, Shanghai, China. Phone: +86-21-63455050; Fax: +86-21-63455090; E-mail: fengyj4806@sohu.com

Submitted February 18, 2012; Accepted for publication July 12, 2012; Epub (www.molmed.org) ahead of print July 12, 2012.

mal transition (EMT) is fundamental to ovarian carcinogenesis and progression (17–19). The notion of epithelial plasticity was described originally during embryonic development as transdifferentiation. An example of this is the critical relationship of the embryonic Müllerian duct to the development of the normal female gonad and reproductive tract (20). In contrast, in the adult, there is debate whether ovarian tumors actually arise from the ovarian surface epithelium or instead from tissues of Müllerian system, which exhibits both epithelial and mesenchymal features (21,22). The elucidation of the epithelial or mesenchymal markers on ovarian cancer stem cells and clarification of the interplay between the EMT and ovarian CSCs might advance our understanding of ovarian tumorigenesis and metastasis, and provide potential new targets for anticancer therapy.

Recently, several groups have reported that the EMT resulted in an increase of a stem cell subset expressing CD44⁺/CD24⁻ surface marker. EMT also exerts a high incidence of tumor formation in breast cancer cells (23). However, it has been indicated recently that a mesenchymal-like phenotype does not correlate with the acquisition of global stem cell/progenitor features (10). This has raised a controversial issue in investigating the relationship between CSCs and the EMT.

In this study, we utilized Hoechst 33342-effluxing assay for detection and enrichment of drug-resistant stemlike SP cells from ovarian cancer patients and ovarian cancer cell lines. We demonstrated that ovarian cancer SP cells were present in patients' ascites and mesenchymally transformed cell lines. When ovarian cancer SP cells were injected with non-SP cells into immunocompromised mice, most SP cells were localized to the xenografted tumor boundary. Stemlike SP cells exhibited decreased adhesive and invasive potential compared with more differentiated non-SP cells. In addition, we provide some evidence supporting the hypothesis that ovarian can-

cer stemlike cells are of epithelial origin and need to undergo the process of EMT concomitant to their transformation. These cells form two distinct pools of cancer cells resulting in tumor heterogeneity, a necessary condition for tumor engraftment and progression.

MATERIALS AND METHODS

Clinical Samples Collection, Cell Culture and Side Population Sorting

The samples were obtained from patients who were diagnosed with ovarian tumors with peritoneal metastasis or ascites and who had not received chemotherapy from April 2011 to September 2011 in the Obstetrics and Gynecology Hospital, Fudan University. Informed consents were obtained from all patients. Detailed pathological information is listed in Supplementary Table S1.

Human epithelial ovarian cancer cell lines, ES-2, SK-OV-3, CAOV-3 and OVCAR-3 were obtained from American Type Culture Collection (Manassas, VA, USA). Another human epithelial ovarian cancer cell line, HO-8910 and its highly metastasizing daughter line HO-8910PM (24), were purchased from the cell bank of Shanghai Institute of Biochemistry and Cell Biology, China. Cells were maintained in DMEM, RPMI 1640, or McCoy's 5A (Gibco, Life Technologies, Carlsbad, CA, USA) containing 10% fetal bovine serum (FBS; Hyclone, Thermo Scientific, Logan, UT, USA) and 1% penicillin/streptomycin (Gibco) according to manufacturer's recommendations. For TGF- β 1 stimulation, 10 ng/mL TGF- β 1 (R&D Systems, Minneapolis, MN, USA) was added and the media were changed every 2 d.

The procedure of Hoechst 33342 staining was described before (25). Briefly, single cells were suspended to 1×10^6 cells/mL in the DMEM/2% FBS and stained with 5 μ g/mL of fluorescence dye Hoechst 33342 (Sigma-Aldrich, St Louis, MO, USA) at 37°C for 90 min. Hoechst 33342-low cells were then analyzed and sorted on ultraviolet laser cytometry (Beckman Coulter, Brea, CA,

USA). Verapamil was added before Hoechst 33342 staining to reliably determine the identity and purity of side population. Detailed information is available in Supplementary Methods.

Flow Cytometry Analysis

Single cells were stained with phycoerythrin (PE)-conjugated antibody against breast cancer resistance protein-1 (BCRP1; EMD Millipore, Billerica, MA, USA) The samples were analyzed on a FACSCalibur (BD Biosciences, San Jose, CA, USA) machine with CellQuest acquisition software. Data analysis was performed using FlowJo Software (Tree Star, Ashland, OR, USA).

For apoptosis analysis, Annexin V-PE Apoptosis Detection Kit (EMD Millipore) was used according to the manufacturer's instruction. Cells were cultured for 4 d without changing medium. Hoechst 33342 dye was added 90 min before incubation with annexin V to identify the SP or non-SP cells. The apoptosis ratio of SP cells and non-SP cells were analyzed by FlowJo Software.

Reverse Transcription-Polymerase Chain Reaction (RT-PCR) Analysis

Total RNA was extracted by using TRIzol reagent (Invitrogen, Life Technologies). One microgram of RNA was used for each reverse transcription (RT) reaction. RT and polymerase chain reaction (PCR) were performed by using PrimeScript RT-PCR Kit (Takara, Shiga, Japan). Quantitative RT-PCR analyses were performed by using ABI PRISM 7500 Fast Real-Time PCR Systems (Applied Biosystems, Life Technologies) and SYBR Green Real-Time PCR Master Mix (Takara). Oligonucleotide primers used are listed in Supplementary Table S2.

In Situ Immunofluorescence Staining

Single cells were cultured in chamber slides and were stained with antibody against vimentin (VIM) (R&D Systems) followed by Rhodamine Red-coupled goat anti-rat IgG (Santa Cruz Biotechnology, Santa Cruz, CA, USA) in the dark. For actin filament (F-actin) stain-

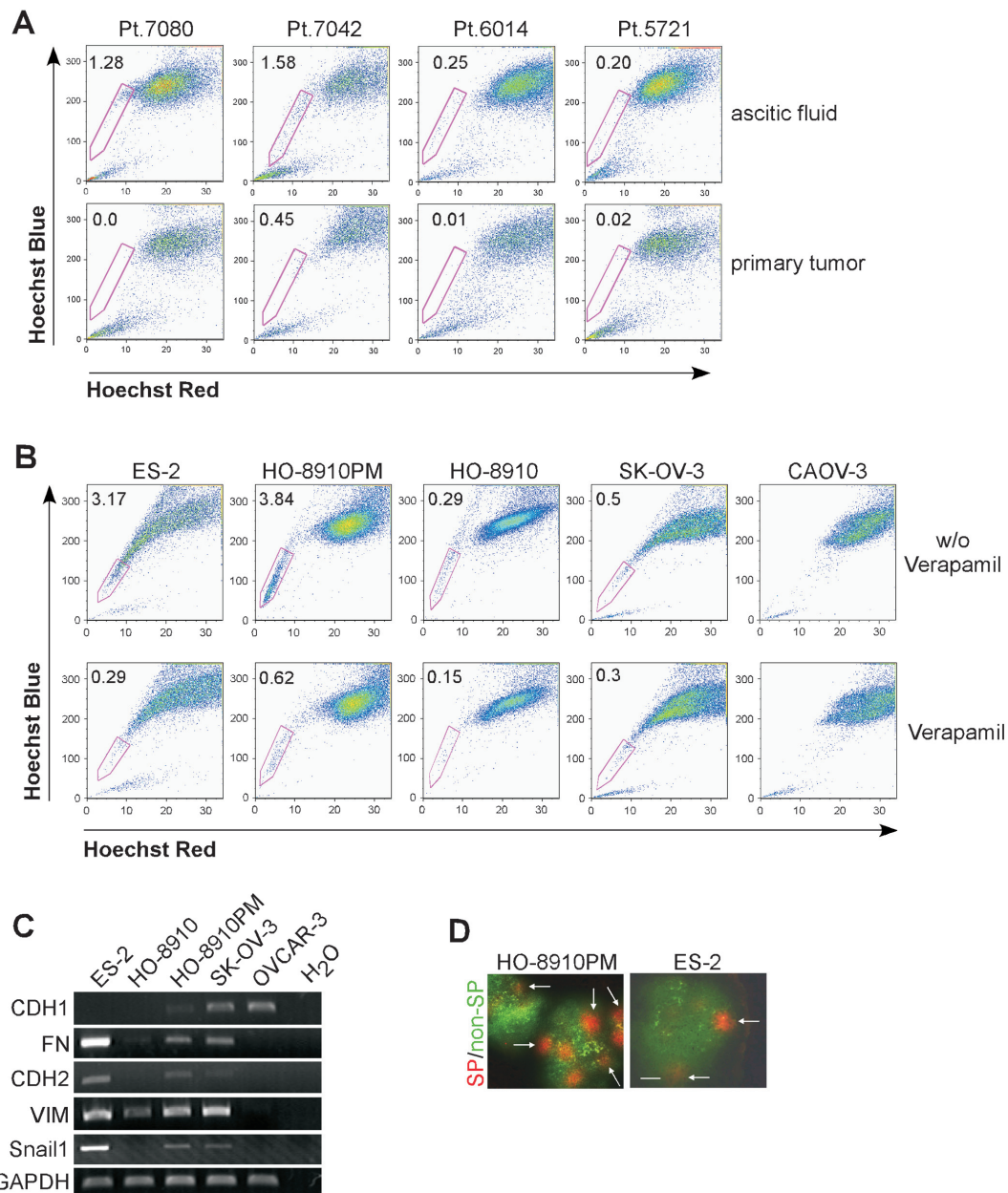


Figure 1. SP component presented in patients' ascitic fluid and localized on tumor boundary. (A) Percentage of SP subpopulation was determined in the cells from ascitic fluid (upper panel) and primary tumor mass (lower panel). Each column of ascitic fluid and primary tumor was obtained from the same patient. (B) Percentage of SP subsets in different ovarian cancer cell lines was determined by flow cytometry after Hoechst 33342 staining. Hoechst 33342-low cell populations were shown to decrease in the presence of verapamil (lower panels). (C) RNA samples from ES-2, HO-8910, HO-8910PM, SK-OV-3 and OVCAR-3 were extracted and analyzed for expression of CDH1, CDH2, FN, Snail1 and VIM by RT-PCR. (D) Localization of SP cells in xenografted tumor. GFP-non-SP cells and RFP-SP cells were isolated and co-injected into nude mice. Xenografted tumor was removed, frozen and sectioned. Expression of GFP and RFP was detected under microscope. Scale bar = 100 μ m.

ing, live adherent cells were stained with 5 μ g/mL Hoechst 33342 for 90 min and then were fixed and stained with Alexa568 conjugated-phalloidin

(Invitrogen) for 30 min. Fluorescence images were acquired by using Leica TCS SP5 MP confocal and multiphoton microscope.

***In Vitro* Colony Formation Assay**

Single cells were cultured in semisolid soft agar or in suspended serum-free media in the presence or absence of

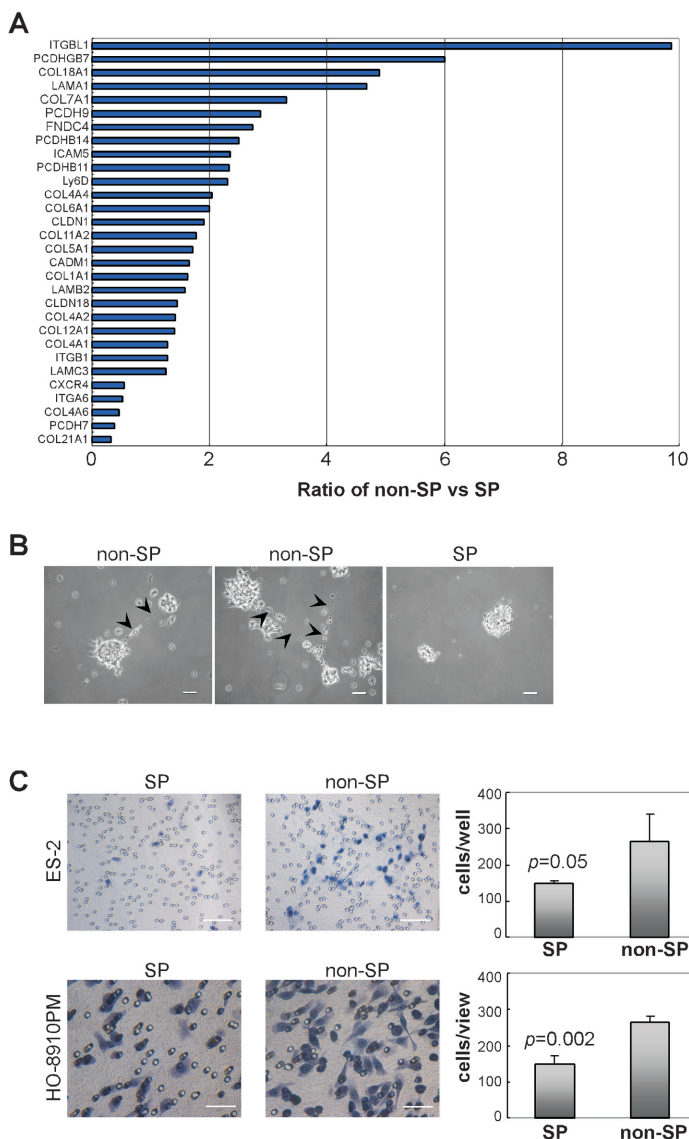


Figure 2. Cell adhesive and invasive capacity of different subpopulations from ovarian cancer cells. (A) Expression of genes relating to cell adhesion in non-SP cells compared with those in SP cells was performed by microarray analysis from HO-8910PM cell line. The graph shows the relative expression level of selected genes in non-SP cells to that in SP cells. Data represent the average of three independent experiments ($p < 0.05$). Detailed information is available in Supplementary Table S3. (B) Sorted ES-2-SP cells and ES-2-non-SP cells were cultured in suspension for 1 wk and were transferred into attaching culture condition. Fine fiberlike structures were observed (arrowed) between non-SP colonies and images were taken no longer than 4 h after colony transfer. Scale bar = 100 μ m. (C) Freshly-sorted SP cells and non-SP cells from ES-2 cells (upper panels) and HO-8910PM cells (lower panels) were suspended in serum-free media and plated onto top chamber of Matrigel-covered micro-pore transwell ($n = 4$). Cells transmigrated into membrane were stained with hematoxylin and counted under microscope. Scale bar = 100 μ m (upper panels), 50 μ m (lower panels).

20 ng/mL recombinant human epidermal growth factor (rhEGF) (R&D Systems) and 10 ng/mL recombinant human basic fibro-

blast growth factor (rhFGF) (R&D Systems) to induce aggregates formation. Details are provided in Supplementary Methods.

Transwell Invasion Assay

Ice-melted Matrigel was diluted with cold DMEM/F12. Fifty μ L of dilution was added to the top chamber and incubated at 37°C for 30 min for gelation. Sorted SP cells and non-SP cells were re-suspended in serum-free DMEM/F12 at the concentration of 10,000 ES-2-derived cells/mL or 150,000 HO-8910PM-derived cells/mL. One hundred μ L of cells was plated in the top well. Six hundred μ L of DMEM/F12 containing 20% FBS was added in the lower chamber of the inner sets. After culturing for 48 h, the invaded cells were stained with hematoxylin and detected under the microscope. Results presented represent quadruplicate experiments and are expressed as mean \pm SD.

Lentiviral Transduction and Snail1 Knockdown

Lentivirus driving GFP or RFP gene was transduced into ES-2 and HO-8910PM cells to generate fluorescence-expressing cells. Snail1-specific shRNA duplex (5'-GCGAG CUGCA GGACU CAAA-3') (26), and a nonspecific control duplex oligo (5'-GGCTA CGTCC AGGAG CGCA-3') were cloned into pGCsi-U6-Neo-GFP lentiviral-based vectors. GFP-positive cells were enriched by fluorescence-activated cell sorting (FACS; Beckman Coulter). Snail1 expression was detected by RT-PCR and Western blotting analysis. Details are provided in Supplementary Methods.

Microarray Assay

Total RNAs were extracted with TRIzol reagent (Invitrogen) and were amplified, hybridized and scanned with Agilent microarray scanner. The significantly enriched genes were selected according to the following criteria: $p \leq 0.05$ and fold change ≥ 2 . Detailed information is available in Supplementary Methods.

In Vivo Xenograft Transplantation

Sorted SP cells and non-SP cells were injected subcutaneously into the dorsal skin of female nude mice (BALB/c-nu/nu) at the age of 4 wks. The engrafted mice were inspected every day for tumorigenicity by visual observation and palpation. When

the tumors were approximately ~1.0 cm in the largest diameter or at 6 months after transplantation, the animals were euthanized by cervical dislocation. The protocol was approved by the institutional committee and complied with the *Guide for the Care and Use of Laboratory Animals* (27).

Statistical Analysis

Data are expressed as mean \pm SD of at least three independent experiments. The significance of difference in the mean value was determined using two-tailed Student *t* test. A *p* value of <0.05 was considered significant.

All supplementary materials are available online at www.molmed.org.

RESULTS

Stemlike SP Cells Presented in Patients' Ascitic Fluid and Localized on Tumor Boundary

The presence of a side population within some ovarian cancer cell lines and primary tumors has been reported previously (14,28). However, the relationship between ovarian cancer SP cell appearance and clinical manifestations remained largely unknown. We analyzed SP percentages in the tumor cells obtained from patients diagnosed with ovarian cancer who had peritoneal metastasis or ascites. We found that SP cells were at a relatively higher level in the cells from ascitic fluid whereas it was relatively low or undetectable in the cells obtained from primary tumor mass of the same patient (Figure 1A). Our findings showed similar results to that of other researchers (29).

To explore the underlying mechanism, it is necessary to purify ovarian cancer SP cells from primary tumors and from ascitic fluid. However, because the cell number is quite low in ascitic fluid, it is methodologically difficult to sort enough primary SP cells for further analysis. Thus, we analyzed additional, previously not characterized human ovarian cancer cell lines, including ES-2, SK-OV-3, CAOV-3, HO-8910 and HO-8910PM, regarding the presence of a side population. There were $>3\%$ of

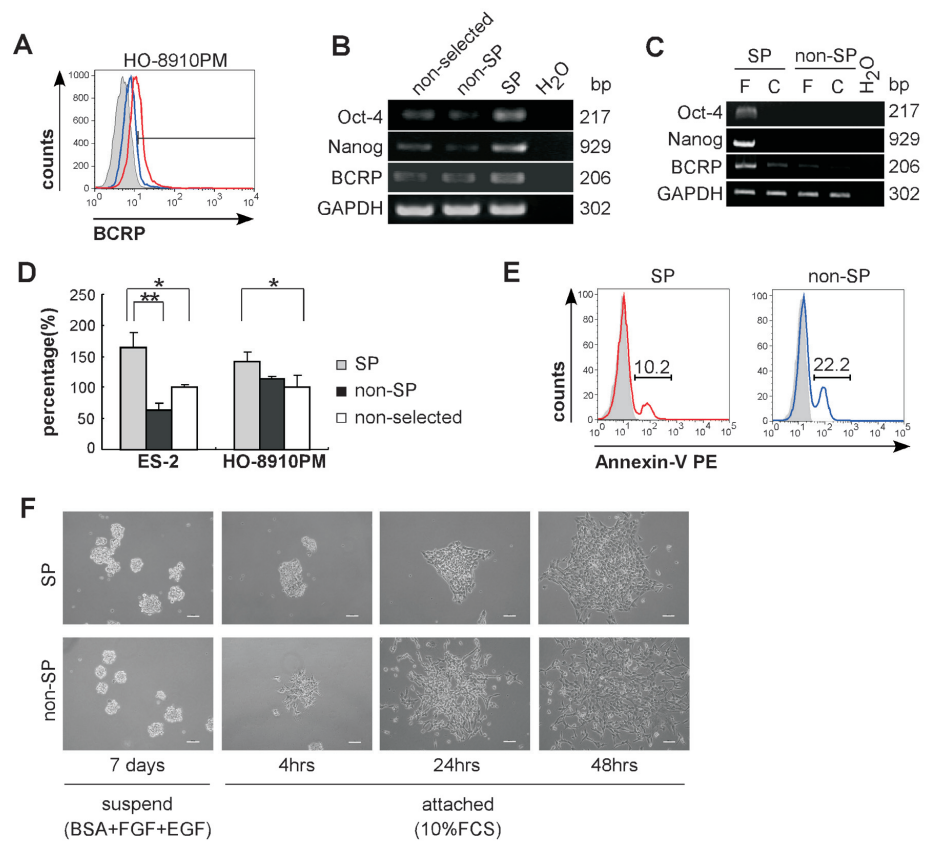


Figure 3. Identification of ovarian cancer stemlike SP cells and characterization of different growth pattern. (A) HO-8910PM-SP cells (red line) and nonselected HO-8910PM cells (blue line) were analyzed for BCRP expression by flow cytometry. The histogram curves were overlaid on relative isotype-matched control antibody (tint). Data are representative of three independent experiments. (B) RNA samples from freshly sorted ES-2-SP cells, freshly sorted ES-2-non-SP cells and nonselected ES-2 cells were isolated and analyzed for expression of Oct-4, Nanog and BCRP by RT-PCR. (C) RNA samples from freshly sorted (F) SP cells, freshly sorted non-SP cells, cultured (C) SP cells and cultured non-SP cells were isolated and analyzed for expression of Oct-4, Nanog and BCRP by RT-PCR (all from HO-8910PM cells). (D) Soft agar colony assay of SP cells and non-SP cells sorted from ES-2 and HO-8910PM lines. After being plated for 14 d, the colonies of diameter $>50 \mu\text{m}$ were counted under a dissecting microscope. Data are defined as the percentage of colony number in SP cells or non-SP cells relative to colony number in nonselected cells. Data represent three independent experiments (**p* < 0.05, ***p* < 0.01). (E) Percentage of apoptotic cells in SP cells (red) or non-SP cells (blue) were determined by PE-conjugated annexin-V staining. The histogram curves were overlaid by the SP cells or non-SP cells respectively without annexin-V staining (tint). (F) Sorted ES-2-SP and ES-2-non-SP cells were cultured in serum-free media in the presence of EGF and FGF-basic for 1 wk in ultra-low attach tissue culture plate (left panels). The suspended spheres were transferred to regular tissue culture plates to induce adhesive growth. The images were taken 4 h, 24 h and 48 h after the spheres had been transferred. Under phase-contrast microscope, the colonies display compact (SP cells) or loose (non-SP cells) appearance after 4 h or 24 h attachment. Scale bar = 50 μm .

cells in ES-2 or HO-8910PM line that exhibited Hoechst-low staining, whereas SP population was at a relatively low level or not detectable in the cell lines of SK-OV-3, CAOV-3 and HO-8910 (Figure 1B). Thus

we used ES-2 and HO-8910PM lines for our ovarian CSCs sorting procedure.

The phenotypical heterogeneity in ovarian cancers has been shown to be intrinsically linked with the transformation

between epithelial and mesenchymal features (30). Based on cell line information, ES-2 is a poorly differentiated ovarian clear cell carcinoma line and HO-8910PM is a highly metastasizing daughter line generated from a poorly differentiated ovarian serous papillary cystadenocarcinoma line (24). Both cell lines expressed lower level of epithelial marker, E-cadherin (CDH1), whereas mesenchymal markers, including N-cadherin (CDH2), fibronectin (FN), VIM and Snail1 were at relatively high levels compared with other cell lines tested (Figure 1C). Of note the different expression of the EMT-related genes were highly correlated with the presence of the SP population in these cell lines.

Tumor cells in ascitic fluid are cells that detach from the primary tumor and disseminate within the abdominal cavity and intensively seed neighboring organs (16). Cell localization might determine the fate of those cells that detach and drop into abdominal cavity. To distinguish different subpopulations within the same tumor tissue, we transduced green fluorescence protein (GFP) or red fluorescence protein (RFP) gene into HO-8910PM and ES-2 cells, respectively. RFP-SP cells and GFP-non-SP cells were isolated by flow cytometry and mixed at the ratio of 4% SP cells and 96% non-SP cells which mimics the ratio of SP to non-SP cells in these cell lines. Total numbers of 2×10^6 of HO-8910PM cells/mouse and 1×10^6 of ES-2 cells/mouse were co-injected subcutaneously into nude mice. The tumors were dissected and detected under microscope. Cells from the SP population (RFP⁺) appeared to grow as a compact group, the majority of which were localized on the boundary of the tumor (see items marked with arrows in Figure 1D), while non-SP cells (GFP⁺) were distributed diffusively in tumor tissues (Figure 1D).

Ovarian Cancer Stemlike Cells Display Decreased Adhesive and Invasive Capacity

When we plated SP cells in regular culture conditions, we found that SP

cells were less able to attach to the culture dish surface than non-SP cells (Supplementary Figure S1A). It indicated that there is an endogenous difference in cell adherent capability between SP cells and non-SP cells. To assess whether the different adherence of ovarian cancer SP cells or non-SP cells are correlated with cell adjacent interaction, we investigated gene expression profiles by microarray analysis. We found that numerous adhesion receptors and extracellular matrix (ECM) transcripts, including integrin- β , intercellular adhesion molecule-5 (ICAM5), cell adhesion molecule-1 (CADM1), claudins, collagens, laminins and FN were downregulated in SP cells compared with those in non-SP cells (Figure 2A, Supplementary Table S3). In addition, when the suspended aggregates were cultured in serum containing medium to grow adherently, minute fiberlike structures were observed between non-SP colonies whereas they were absent in SP derived colonies (Figure 2B). This again indicates that ovarian cancer SP cells exhibit less potential to interact with each other and have reduced adherence capacity to the ECM.

In cancer cells, F-actins are organized into bundles dynamically assembling and disassembling for cells to move and change shape (31). By phalloidin staining, we observed that in Hoechst 33342-positive ovarian cancer non-SP cells, F-actins were seen as organized bundles whereas these structures were less apparent in Hoechst 33342-negative SP cells (Supplementary Figure S1B). To further quantify the mobility and invasiveness of different ovarian cancer cell subpopulations, isolated ovarian cancer SP cells and non-SP cells were plated into upper chamber of a micropore transwell, which was covered with gelled Matrigel matrix. As shown in Figure 2C, more non-SP cells from ES-2 or HO-8910PM lines were detected to invade into Matrigel matrix after 48 h in culture, indicating that freshly-sorted ovarian cancer SP cells are less invasive than non-SP cells.

Characterization of Different Growth Patterns between SP Cells and Non-SP Cells

SP cells in various cancers have demonstrated tumorigenicity and behave with stemlike features (14,32–36). To see if SP cells from ES-2 and HO-8910PM cell lines exhibit some stem cell like features *in vitro*, we sorted Hoechst 33342-low cells for analysis of Oct-4 and Nanog expression. BCRP1, a drug efflux protein relating to cellular drug resistance (12), was analyzed by FACS and RT-PCR. Sixty-three percent of HO-8910PM SP cells expressed BCRP1 whereas expression in non-SP cells was 3.99% (Figure 3A). SP cells from ES-2 or HO-8910PM cell lines exhibited marked elevation in BCRP1 expression at the mRNA level, as well as in expression of pluripotent genes, Oct-4 and Nanog (Figures 3B, C). SP cells from both cell lines showed higher colony forming capability in semi-solid soft agar than non-SP cells at equal initiating cell numbers (Figure 3D). In addition, SP cells showed less tendency to cause apoptosis than non-SP cells (10.2% versus 22.2%) indicating that cancer stemlike cells are more resistant to environmental pressure (Figure 3E).

A limited dilution assay for single-cell derived colony formation was used to further investigate the cell proliferation. Single SP cells were able to form suspended aggregated colonies within 4 d and continued to proliferate even after 2 wks (Supplementary Figure S2A) whereas non-SP cells failed to sustain cell growth beyond 2 wks of culture procedure. The frequency of Hoechst-effluxing cells was reassessed after culturing procedure. Ninety percent of SP cells differentiated into non-SP cells while 10% of cultured-SP cells retained the capability to efflux the Hoechst dye, indicating that ovarian cancer SP cells can generate both SP and non-SP cells. After 2 wks of cultivation, 1% to 2% of cultured non-SP cells regained Hoechst-effluxing capability, indicating that a small fraction of non-SP cells can reestablish SP cell phenotype. However, as shown in Supplementary Figure S2B, the percentage of Hoechst-

Table 1. Tumorigenicity of HO-8910PM cells at subcutaneous injection site.

Group	Tumors incidence/ number of injections		
	2×10^5	1×10^5	5×10^4
SP	3/3	3/3	5/5
non-SP	3/3	2/3	1/5

effluxing cells in cultured non-SP cells was far less than in cultured SP cells (2% versus 10%), indicating that ovarian cancer SP cells possess a higher capability to generate Hoechst-effluxing cells than non-SP cells. Moreover, when the cells were treated with mitoxantrone, one of the chemotherapeutic agents used to treat patients with ovarian cancer (37), colony formation was inhibited by 45% in ES-2 SP cells whereas the ES-2 non-SP cells showed 65% inhibition (Supplementary Figure S2C). Thus, SP cells in ES-2 and HO-8910PM lines display more pluripotent capacity and less sensitivity to chemotherapy than non-SP cells.

To assess the tumorigenicity of ovarian cancer SP cells *in vivo*, sorted SP cells or non-SP cells from ES-2 or HO-8910PM cells were injected into nude mice. SP cells, either freshly sorted or cultured for 2 wks, were shown to have a higher efficacy to form tumors *in vivo* compared with non-SP cells at the equal initiating number of cells/mouse (Tables 1 and 2).

To gain more detailed information about the biological nature of ovarian cancer SP cells, we took a closer look at the cell behavior in *in vitro* conditions. SP cells from both lines formed characteristic circular, cobblestonelike colonies in serum-containing medium. In contrast, non-SP cells from both lines immediately attached to the bottom of the culture dishes and grew sparsely, with a branched cytoplasm in appearance (Supplementary Figures S1A, D).

To mimic the growth pattern of ovarian cancer cells in ascites, SP cells and non-SP cells were inoculated in ultra-low attachment plates in the presence of EGF and bFGF in serum-free media to induce anchorage-independent, autonomous, three-dimensional spheroids. Nonadherent

Table 2. Tumorigenicity of ES-2 cells at subcutaneous injection site.

Group	Tumors incidence/number of injections			
	$(0.75-1) \times 10^5$	1×10^4	1×10^5	1×10^2
Cultured SP	4/5	4/5	3/5	3/5
Cultured non-SP	5/5	5/5	3/5	0/5
Nonselected	5/5	5/5	3/5	1/5

spherical clusters of cells were observable 1 wk after plating, with no visual difference between the two subpopulations under phase-contrast microscope (Figure 3F, left panel). However, after transfer to serum-containing medium, the spheroids shortly adhered to the regular tissue culture bottom with a distinct compact or loose appearance. Seventy-two percent of ES-2 SP-derived spheroids, compared with 44% of those from non-SP cells, were compact with a relatively confined margin shortly after attachment ($p < 0.001$). Within 4 h, most non-SP spheroids possessed fingering tumor fronts beyond the borders of the main tumor clusters, in which majority of cells acquired a fibroblast-like, elongated spindle-shaped appearance with loose cell:cell interaction. In contrast, SP spheroids were less capable of stretching and did not form satellite structures until 48 h after attachment (Figure 3F). To further assess cell infiltrative capability in extracellular matrix, the percentage of colony diameter $>50 \mu\text{m}$ in semisolid agar was estimated under the microscope. Similar to that observed in serum-free condition, colonies from non-SP cells were looser and more widespread suggesting further migration distance of non-SP cells compared with SP cells (Supplementary Figure S2E).

Heterogeneous Expression of Epithelial and Mesenchymal Markers on Ovarian Cancer Subpopulations

We detected that ovarian cancer non-SP cells displayed a much higher adherent capacity than SP cells. This raises the possibility that ovarian CSCs need to undergo an endogenous transformation from SP cells into non-SP cells, to induce a more invasive phenotype and orchestrate cancer cell engraftment. Compared to SP cells, the growth pattern of ovarian cancer

non-SP cells, including fibroblast-like morphology, invasive capacity into ECM and increased expression of adherent junctions indicates that transformation from SP cells to non-SP cells allows the cells to acquire a migratory mesenchymal behavior. This acquired behavior benefits their integration into surrounding tissue.

To determine if there is any change in the expression profile of epithelial or mesenchymal markers between ovarian cancer SP and non-SP cells, we examined the expression of genes known to regulate the EMT process, such as Snail1, Snail2, S100A4, SIP1, keratins and SMADs. The mesenchymal markers (Snail1, Snail2 and S100A4) were shown to have a lower expression while epithelial markers (keratin8, keratin15, SMAD2 and SMAD3) had a higher expression in SP cells compared with non-SP cells (Figure 4A).

We then investigated the expression pattern of VIM (38), the essential regulator of the EMT in freshly sorted SP cells, freshly sorted non-SP cells and cultured SP cells from HO-8910PM cells. We found that VIM was only detectable on the cell surface in SP cells whereas in non-SP cells, VIM was found diffusely distributed both in the cytoplasm and on the cell membrane. After 3 d in culture, proliferating SP cells underwent changes in cell morphology. They displayed elongation in shape and expression of VIM was spatially distributed into the cytoplasm as well as on the cell membrane (Figure 4B). In addition, we detected the dynamic changes in the expression of EMT-related genes after culturing of sorted cell subsets. Freshly sorted ES-2-SP cells expressed lower levels of mesenchymal markers, including CDH2, FN, VIM and Snail1 than non-SP cells. However, during the culture in serum-free medium and subsequently in serum-containing

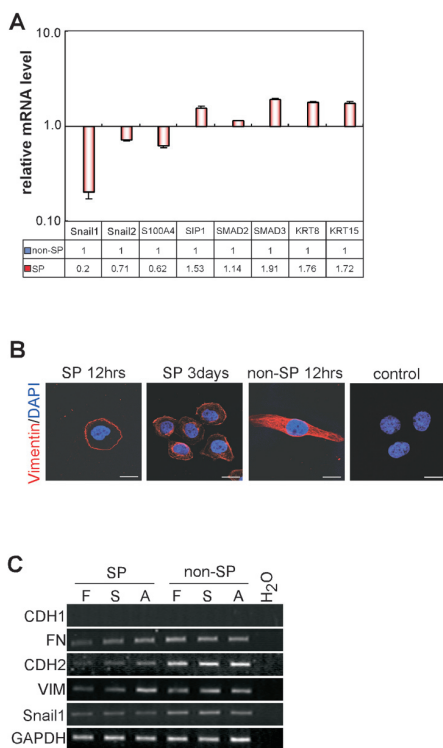


Figure 4. Different expression of epithelial and mesenchymal markers. (A) Expression of genes encoding Snail1, Snail2, S100A4, SIP1, SMAD2, SMAD3, KRT8 and KRT15 in HO-8910PM-SP cells relative to non-SP cells were determined by real-time RT-PCR ($p < 0.05$). (B) Sorted HO-8910PM-SP cells and non-SP cells were cultured for 12 h or 3 d and subsequently stained with antibody against VIM followed by Rhodamine Red-coupled goat anti-rat IgG or stained only with Rhodamine Red-coupled goat anti-rat IgG (control). Scale bar = 15 μ m. (C) RNA samples from ES-2 SP or non-SP cells were extracted and analyzed for expression of CDH1, CDH2, FN, Snail1 and VIM by RT-PCR. Samples were collected from freshly-sorted cells (F), cells cultured in suspended serum-free media in the presence of EGF and FGF-basic for 1 wk (S), or cells cultured in suspension for 1 wk and then plated in serum containing medium for additional 1 wk (A).

medium, the expression levels of FN, VIM and CDH2 increased in the cells derived from the SP population, whereas no obvious changes were observed in cells from non-SP cells (Figure 4C). The heterogeneity of ovarian cancer SP cells and non-SP cells during 2 wks in culture may

explain the increased adherence during transformation from SP cells to non-SP cells which is related, at least in part, to the EMT.

TGF- β 1 Enhances EMT-Related Gene Expression during Ovarian Cancer Stemlike Cell Differentiation

It has been demonstrated that TGF- β family members are involved in the regulation of embryonic development and cancer initiating cells (39). TGF- β 1 has been shown to be the main factor resulting in a more invasive phenotype in epithelial tumors via the EMT process (40), and to repress the transcription of BCRP1 / ABCG2 resulting in decrease of SP population (41). To determine the impact of TGF- β 1 on ovarian cancer SP cells, we cultured HO-8910PM cells in the presence of TGF- β 1. After treatment with TGF- β 1 for 3 d, the frequency of SP cells was reduced markedly from 2.25% to 0.39% (Figure 5A), which is consistent with the previous findings (41).

To identify molecular regulators of the TGF- β 1 mediated transformation of ovarian cancer SP cells, microarray analysis was performed to compare the gene expression pattern on freshly-sorted SP cells, freshly-sorted non-SP cells, TGF- β 1-stimulated SP cells (TSS) and human fibroblasts (HF). A cluster analysis of orthologous genes in various cell groups was performed based on the gene expression profiles. The analysis of expressing genes showed that freshly sorted SP cells and TGF- β 1-stimulated SP cells clustered together. Freshly sorted non-SP cells and HF also were clustered together. In contrast, SP cells and non-SP cells were clustered separately (Figure 5B). These results again point to a different nature of these subpopulations even within the same tumor cell line.

We further performed real-time PCR analysis to investigate the variation trend of EMT-related genes on different subpopulations. TGF- β 1 was added to stimulate the cells and expression levels of Snail1, Snail2 and CDH2 were determined at different time points during stimulation. We found that TGF- β 1 effectively stimulated

transformation of HO-8910PM SP cells into mesenchymal features. During 2 wks of cultivation, expression of CDH2, Snail1 and Snail2 in HO-8910PM SP cells were increased significantly in the presence of TGF- β 1 compared with those in the absence of TGF- β 1 (Supplementary Figure S3). Snail1 was more highly regulated in TGF- β 1-stimulated SP cells compared with TGF- β 1-stimulated non-SP cells during the entire course of culture, whereas the differences in Snail2 or CDH2 were not so apparent (Figure 5C). CDH1 was expressed at low levels on ES-2 and HO-8910PM cells (Figure 4C). However, expression of CDH2, which implies CDH1 to CDH2 switch (EN switch), increased and the highest expression was observed on d 13 of stimulated non-SP cells (Figure 5C).

Additionally, we found that actin filaments in non-SP cells were stained as well-oriented stress fibers or three-dimensional networks in the presence or absence of TGF- β 1. However, as shown in Figure 5D, F-actin in freshly sorted SP cells displayed lower, unbundled expression. After differentiation for 3 d, actins in SP cells were barbed, but still less organized and more disorderly compared with those in non-SP cells. TGF- β 1 stimulated actin polymerization in SP cells and the cells grew with more polarization and extension during the stimulation.

Inhibition of Snail1-Regulated EMT Reduced Invasiveness of Ovarian Cancer Stemlike Cells and Tumorigenicity

We proceeded to determine whether the EMT process has an impact on ovarian cancer stem cell maintenance. Snail1 has been detected as an important regulator of the EMT (42) and expressed at a higher level in ovarian cancer non-SP cells compared with SP cells (Figure 4A). We designed a shRNA lentiviral construct specifically against human Snail1 gene and transduced it into HO-8910PM cells. Expression of Snail1 was efficiently suppressed at both mRNA and protein levels (Figures 6A, B). As anticipated, the resulting cells lost their fibroblast-like appearance (Figure 6C), increased the ex-

pression of mRNA encoding epithelial markers (CDH1), and decreased that of encoding mesenchymal markers (CDH2 and FN) (see Figures 6A, B). These results indicate functional suppression of cellular mesenchymal transformation.

We further detected that the percentage of SP cells was decreased markedly after Snail1 downregulation ($0.38 \pm 0.06\%$ in shSnail1 cells compared with $3.03 \pm 0.05\%$ in vector control cells, $p < 0.01$) (Figure 6D). It indicates that Snail1-regulated EMT is crucial to ovarian cancer SP cell maintenance. This is consistent with our findings that ovarian cancer SP cells were present in more mesenchymally transformed cell lines (Figures 1B, C). In addition, shSnail1 cells displayed an affected invasive capability compared with the cells transduced with a control vector (Figure 6E). Tumorigenicity was reduced after Snail1 inhibition (Table 3). We performed an annexin-V assay to see whether regulation of Snail1 induces SP cell apoptosis and thus results in reduced tumorigenicity. As demonstrated in Figure 6F, shSnail1-SP cells consistently showed less annexin-V affinity frequency than shSnail1-non-SP cells (3.8% versus 8.4%), indicating that shSnail1-SP cells retained a higher resistance to apoptosis than shSnail1-non-SP cells. It clarified that inhibition of Snail1-regulated EMT in ovarian cancer cells results in not apoptosis but suppression of cellular invasiveness both *in vitro* and *in vivo*.

DISCUSSION

CSCs have been documented in a variety of neoplasm, and the EMT has been indicated as a program required for cellular remodeling during embryogenesis, wound healing and acquisition of malignant traits (43). Recent studies have described a convergence of both lines of research, indicating that CSCs occur in part as a result of EMT (23,44). Some studies reported that the EMT resulted in increased numbers of CSCs with mesenchymal phenotype and metastatic properties, the majority of which were performed on breast cancer stem cells selected by CD44⁺/CD24⁻ expression (23,45). In con-

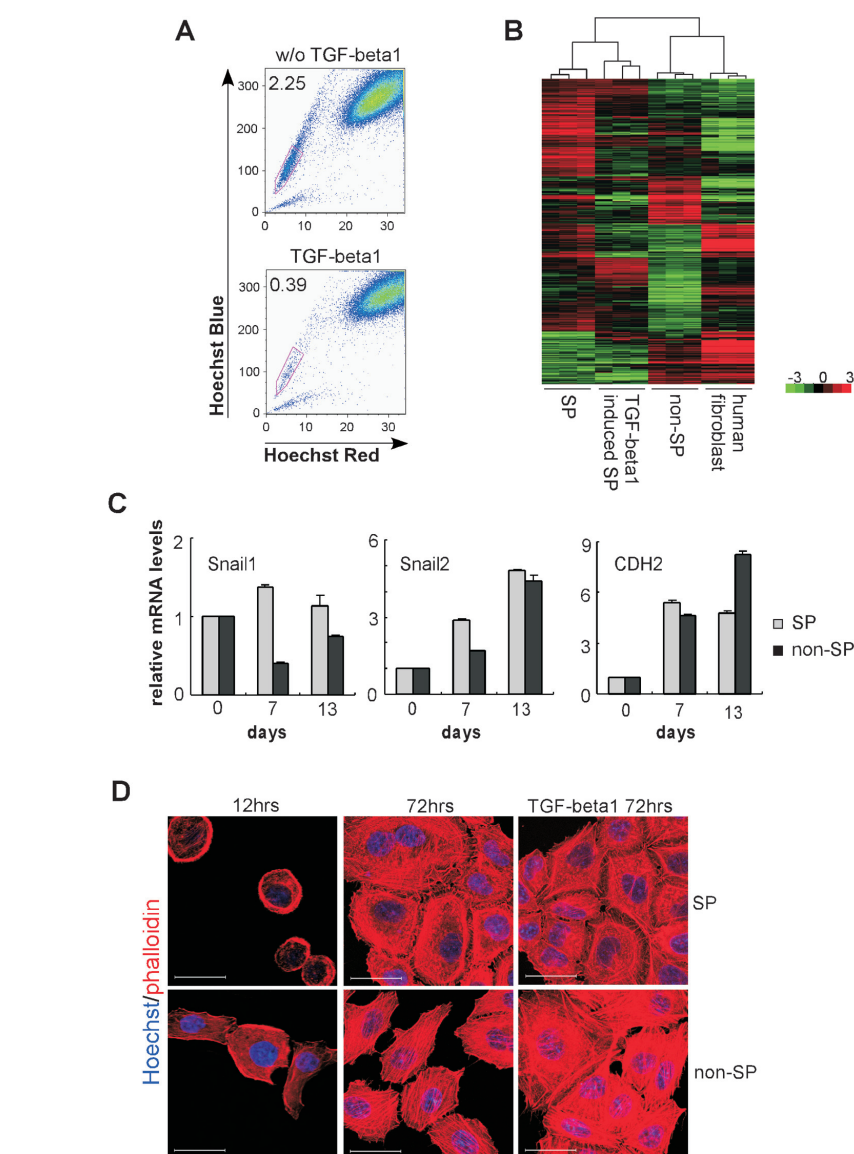


Figure 5. Gene expression profiles during TGF- β 1 stimulation. (A) SP cell content was determined by FACS analysis in untreated cells or cells treated with TGF- β 1 for 72 h (all from HO-8910PM cells). (B) Microarray analyses were performed to compare gene expression profiles of freshly sorted SP cells, freshly sorted non-SP cells, TGF- β 1 induced SP cells (all from HO-8910PM cells) and human fibroblast cell line, HS-27. The hierarchical cluster analyses of orthologous genes were performed based on signal ratio. (C) Expression of Snail1, Snail2 and CDH2 in SP cells or non-SP cells during TGF- β 1 stimulation (d 7, d 13) relative to unstimulated level (d 0) was determined by real-time RT-PCR (all from HO-8910PM cells). (D) Sorted SP cells or non-SP cells from HO-8910PM were cultured for 12 h and 72 h, in the presence or absence of TGF- β 1. Live cells were stained with Hoechst 33342 and subsequently fixed and co-stained with Alexa568 conjugated-phalloidin. Scale bar = 30 μ m.

trast, other studies indicated that stem cell/progenitor properties reside predominantly within normal epithelial breast basal subpopulation, which was sorted by

EpCAM. They proposed that generation of mesenchymal-like cells via EMT in normal basal breast cells and claudin-low breast cancers reflects cellular differentia-

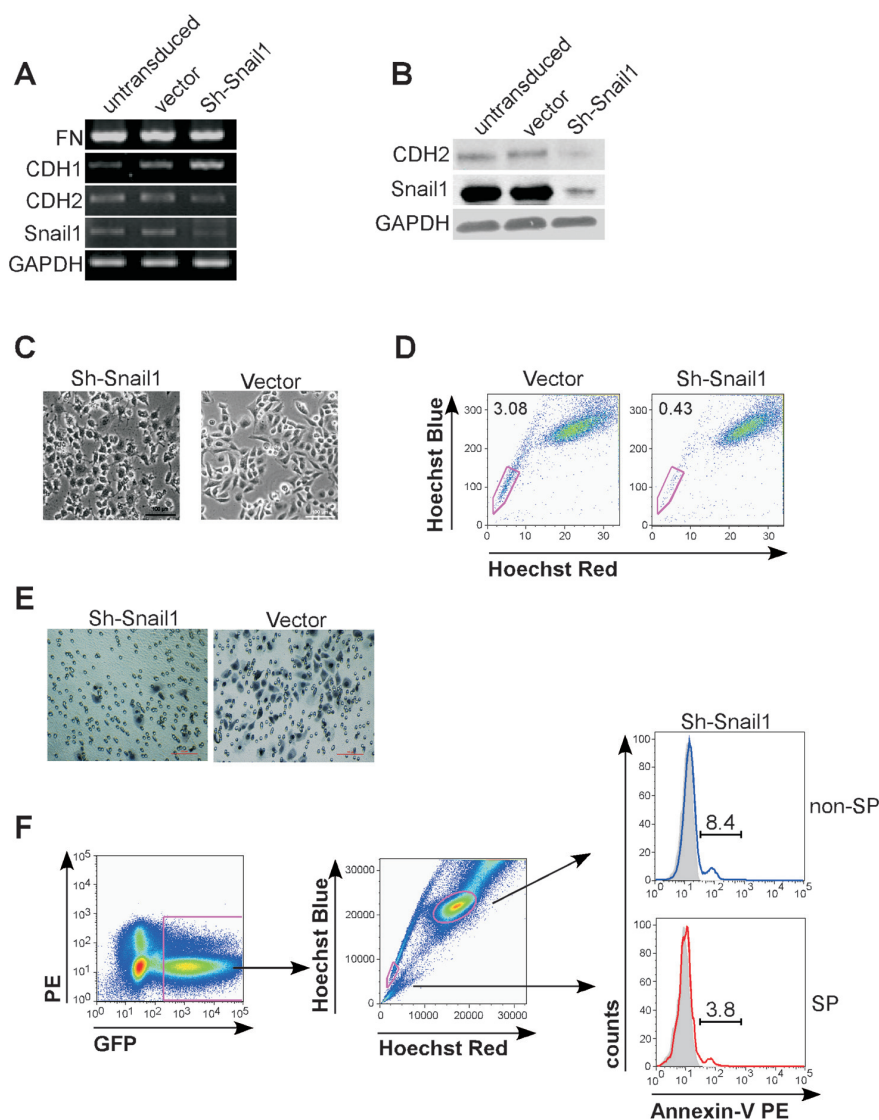


Figure 6. Downregulation of Snail1 decreased ovarian cancer stemlike cell percentage and inhibited their invasive capacity. Untransduced cells, and cells transduced with control vector or shSnail1 (all from HO-8910PM cells) were analyzed for expression of CDH1, CDH2, FN and Snail1 by RT-PCR (A), Western blotting assay (B) and were detected under microscope (C). Scale bar = 50 μ m. (D) SP cells were determined by FACS analysis in HO-8910PM cells transduced with control vector or shSnail1 lentivirus. (E) HO-8910PM cells transduced with control vector or shSnail1 were suspended in serum-free media and plated onto top chamber of Matrigel-covered micropore transwell. Cells migrated into membrane were stained with Hematoxylin and counted under microscope. Scale bar = 100 μ m. (F) Experimental scheme for FACS analysis of apoptosis in lentiviral transduced shSnail1 cells. GFP-positive (transduced) cells were analyzed (left) and gated as SP cells and non-SP cells (middle). Percentage of apoptotic cells in GFP-positive SP cells (red) or GFP-positive non-SP cells (blue) were determined by PE-conjugated annexin-V staining (right). The histogram curves were overlaid by the SP cells or non-SP cells without annexin-V staining (tint).

tion (10). These two lines of reports reflect a controversy in investigating the relationship between CSCs and the EMT.

Ovarian cancers, a heterogeneous group of tumors, consist of various pathologic subtypes and show different clinical be-

Table 3. Subcutaneous tumorigenicity of Sh-Snail1 HO-8910PM cells.

Group	Tumors incidence/ number of injections		
	2×10^6	1.5×10^6	1×10^6
Vector control	6/6	6/6	6/6
Sh-Snail1	6/6	3/5	0/6

haviors. The question of whether ovarian cancers occur from ovarian epithelium or instead from Müllerian extraovarian tissues which possess both epithelial and mesenchymal properties, has been discussed for years (21,46). The uncertain pathological origin of ovarian cancers challenges our understanding of these cancers (29,47). The characterization of ovarian CSCs might help to answer this question.

There is increasing evidence by the isolation of tumor subsets for the existence of CSCs in ovarian cancers. A number of cell surface markers have proven to be useful for the isolation of subsets enriched for ovarian CSCs, including CD133⁺ (48,49), CD133⁺ ALDH⁺ (11), CD44⁺ CD117⁺ (50), EpCAM (51) and Hoechst 33342 exclusion of the SP cells (14). Among them, the presence of SP cells has allowed identification of cancer stemlike cells and reflects a mechanism of oncogenesis and drug resistance on the basis of drug efflux proteins (12,14). Additionally, the markers mostly used for sorting ovarian CSCs, CD44 and CD133, also are markers representative of mesenchymal lineage (52,53). The population which was sorted by expression of CD44 and CD133 might gate out an epithelial pluripotent subpopulation. It would result in a similar issue if CSCs were sorted by using the epithelial marker, EpCAM (10). Whether ovarian CSCs express epithelial or mesenchymal markers remains largely unknown.

In this study, we utilized the Hoechst 33342 effluxing assay instead of surface markers to purify ovarian cancer stemlike cells. This technique excludes possible cellular differences which result from sorting methods using epithelial or mesenchymal markers. It has been indicated that a very small population of ovarian cancer SP cells has the potential to initiate tumor

growth *in vivo*. As demonstrated previously by others (14,25), we report here that SP components from ovarian cancer cells exhibited some specific stemlike properties compared with non-SP cells, including self-renewal capacity, pluripotent genes expression and tumorigenicity. Ovarian cancer SP cells showed higher drug resistance than non-SP cells. In addition, we showed that ovarian cancer SP cells expressed epithelial markers, including KRT8, KRT15 and round-shaping growth pattern, whereas the expression of mesenchymal markers, CDH2 and VIM were at a decreased levels compared with non-SP cells from the same cancer cell line. Ovarian cancer SP cells grew clonally as a compact group, while non-SP cells were distributed diffusively in tumor tissues. Thus, we provide the evidence that ovarian cancer stemlike SP cells exhibits epithelial features.

It is thought that ovarian cancer cells metastasize through a passive mechanism once the cancer cells have detached as single cells or clusters from the primary ovarian tumor (16,17,54). We present data here that, from the same patient, percentages of ovarian cancer SP component in ascitic fluid were relatively higher than those in primary tumor. The reduced expression of various integrins and components of the extracellular matrix on ovarian cancer SP cells, such as FN, laminin and collagen suggest that the adhesive interaction between ovarian cancer stemlike cells and the surrounding microenvironment is delicate. In addition, we found that ovarian cancer SP cells were localized to xenografted tumor boundary. These results indicate that SP cells exert an important role in ovarian cancer progression on the basis of their delicate interaction with surrounding microenvironment and anatomical localization in tumors. The distinct cellular subpopulations within the same cell lines determinate the heterogeneous nature in tumors.

To execute the process of tumor progression, ovarian cancer cells need to be engrafted and the process is niche-dependent and governed by an underlying molecular mechanism (55,56). We showed that freshly

sorted ovarian cancer SP cells behaved with a reduced invasive capability. In contrast, ovarian cancer non-SP cells, presumably more differentiated tumor cells, possessed higher migratory and invasive properties and were more able to interact with the surrounding microenvironment than stemlike SP cells. In addition, transformation of ovarian cancer SP cells into non-SP cells was orchestrated by genes associating with the EMT program, such as Snails, S100A4, SMADs, keratins and adherents, and facilitated execution of most steps of the invasion cascade by induction of F-actin stress fibers. This suggests that the differentiation of ovarian CSCs is dependent on the genes turning on or off, and is related to the endogenous process of EMT. In contrast to the results from the CD44⁺/CD24⁻ breast cancer stemlike cells (23), our data indicates that transformation of ovarian cancer stemlike SP cells into more differentiated non-SP cells is concomitant to the EMT process.

Our *in vivo* data also demonstrated that the inhibition of the transformation from epithelial phenotype into more mesenchymal phenotypes markedly reduced ovarian cancer cell engraftment. It indicated that in ovarian cancer tumorigenicity, mesenchymal non-SP cells displayed enhanced invasive features while epithelial SP cells enabled sustained tumor growth and hence, both cell types regulate cancer progression. On the basis of increasing interaction with the surrounding environment which was generated by differentiated cells, ovarian cancer SP cells were evidently more tumorigenic than non-SP cells with an adaptive change involving, at least in part, the process of EMT.

We have demonstrated here that the ovarian cancer cell lines contained higher percentage of SP cells and also expressed mesenchymal traits and typical mesenchymal gene expression patterns. It indicates that incidence of ovarian cancer SP cells in different cell lines is highly correlated with the expression of the EMT-related genes. Inhibition of the EMT process by Snail1 silencing decreased the ovarian cancer SP cell frequency, affected their invasive capacity and thus resulted

in reduced tumorigenicity *in vivo*. Taking these together, it again emphasizes the heterogeneity even within the same cancer cell line and demonstrates that the Snail1-regulated EMT is essential to epithelial ovarian CSC maintenance.

CONCLUSION

Collectively, our findings indicate the flexibility of the niche function and present an intriguing model for how epithelial ovarian cancer stem cells, which have accumulated mutations over time, may evolve their pathological behaviors. It supports a growing body of evidence that the CSC-containing population in some cancers do reestablish the heterogeneity via the EMT, which may be responsible for drug resistance, tumor progression and metastasis. Future investigations need to address how to aim this mechanism as a potential target in anticancer therapy.

ACKNOWLEDGMENTS

We thank Guoping Zhang (Fudan University) for his assistance of SP cell sorting. We thank David Scadden and Anne Kathryn Goodman (Massachusetts General Hospital, Harvard Medical School, Boston, MA, USA) for critical reading of this manuscript. This study was supported by the National Basic Research Program of China 2011CB910404 (TC), National Natural Science Foundation of China 81070399 (TC), Program for New Century Excellent Talents in University NCET-09-0307 (TC), Foundation from Science and Technology Commission of Shanghai Municipality 11JC1401501 (HJ).

DISCLOSURES

The authors declare they have no competing interests as defined by Molecular Medicine, or other interests that might be perceived to influence the results and discussion reported in this paper.

REFERENCES

1. Park CH, Bergsagel DE, McCulloch EA. (1971) Mouse myeloma tumor stem cells: a primary cell culture assay. *J. Natl. Cancer Inst.* 46:411–22.
2. Hamburger A, Salmon SE. (1977) Primary bioassay of human myeloma stem cells. *J. Clin. Invest.* 60:846–54.

3. Kennedy JA, Barabe F, Poepl AG, Wang JC, Dick JE. (2007) Comment on "Tumor growth need not be driven by rare cancer stem cells." *Science*. 318:1722; author reply 1722.
4. Kelly PN, Dakic A, Adams JM, Nutt SL, Strasser A. (2007) Tumor growth need not be driven by rare cancer stem cells. *Science*. 317:337.
5. Al-Hajj M, Wicha MS, Benito-Hernandez A, Morrison SJ, Clarke MF. (2003) Prospective identification of tumorigenic breast cancer cells. *Proc. Natl. Acad. Sci. U. S. A.* 100:3983–8.
6. Ricci-Vitiani L, et al. (2007) Identification and expansion of human colon-cancer-initiating cells. *Nature*. 445:111–5.
7. Hermann PC, et al. (2007) Distinct populations of cancer stem cells determine tumor growth and metastatic activity in human pancreatic cancer. *Cell Stem Cell* 1:313–23.
8. Li C, et al. (2007) Identification of pancreatic cancer stem cells. *Cancer Res*. 67:1030–7.
9. Schatton T, et al. (2008) Identification of cells initiating human melanomas. *Nature*. 451:345–9.
10. Sarrjo D, Franklin CK, Mackay A, Reis-Filho JS, Isacke CM. (2012) Epithelial and mesenchymal subpopulations within normal basal breast cell lines exhibit distinct stem cell/progenitor properties. *Stem Cells*. 30:292–303.
11. Silva IA, et al. (2011) Aldehyde dehydrogenase in combination with CD133 defines angiogenic ovarian cancer stem cells that portend poor patient survival. *Cancer Res*. 71:3991–4001.
12. Haraguchi N, et al. (2006) Characterization of a side population of cancer cells from human gastrointestinal system. *Stem Cells* 24:506–13.
13. Hirschmann-Jax C, et al. (2004) A distinct "side population" of cells with high drug efflux capacity in human tumor cells. *Proc. Natl. Acad. Sci. U. S. A.* 101:14228–33.
14. Szotek PP, et al. (2006) Ovarian cancer side population defines cells with stem cell-like characteristics and Mullerian Inhibiting Substance responsiveness. *Proc. Natl. Acad. Sci. U. S. A.* 103:11154–9.
15. Zhou BB, et al. (2009) Tumour-initiating cells: challenges and opportunities for anticancer drug discovery. *Nat. Rev. Drug. Discov.* 8:806–23.
16. Lengyel E. (2010) Ovarian cancer development and metastasis. *Am. J. Pathol.* 177:1053–64.
17. Elloul S, et al. (2005) Snail, Slug, and Smad-interacting protein 1 as novel parameters of disease aggressiveness in metastatic ovarian and breast carcinoma. *Cancer*. 103:1631–43.
18. Jin H, et al. (2010) Snail is critical for tumor growth and metastasis of ovarian carcinoma. *Int. J. Cancer*. 126:2102–11.
19. Ahmed N, Thompson EW, Quinn MA. (2007) Epithelial-mesenchymal interconversions in normal ovarian surface epithelium and ovarian carcinomas: an exception to the norm. *J. Cell Physiol.* 213:581–8.
20. Oktem O, Oktay K. (2008) The ovary: anatomy and function throughout human life. *Ann. N. Y. Acad. Sci.* 1127:1–9.
21. Dubeau L. (2008) The cell of origin of ovarian epithelial tumours. *Lancet Oncol* 9:1191–7.
22. Kurman RJ, Visvanathan K, Roden R, Wu TC, Shih Ie M. (2008) Early detection and treatment of ovarian cancer: shifting from early stage to minimal volume of disease based on a new model of carcinogenesis. *Am. J. Obstet. Gynecol.* 198:351–6.
23. Mani SA, et al. (2008) The epithelial-mesenchymal transition generates cells with properties of stem cells. *Cell*. 133:704–15.
24. Shenhua X, et al. (1999) Establishment of a highly metastatic human ovarian cancer cell line (HO-8910PM) and its characterization. *J. Exp. Clin. Cancer Res*. 18:233–9.
25. Goodell MA, Brose K, Paradis G, Conner AS, Mulligan RC. (1996) Isolation and functional properties of murine hematopoietic stem cells that are replicating in vivo. *J. Exp. Med.* 183:1797–806.
26. Fujita N, et al. (2003) MTA3, a Mi-2/NuRD complex subunit, regulates an invasive growth pathway in breast cancer. *Cell*. 113:207–19.
27. Institute of Laboratory Animal Resources; Commission on Life Sciences; National Research Council. (1996) *Guide for the Care and Use of Laboratory Animals*. Washington (DC): National Academy Press. [cited 2012 Oct. 2]. Available from: http://www.nap.edu/openbook.php?record_id=5140
28. Moserle L, et al. (2008) The side population of ovarian cancer cells is a primary target of IFN- α antitumor effects. *Cancer Res*. 68:5658–68.
29. Hosonuma S, et al. (2011) Clinical significance of side population in ovarian cancer cells. *Hum. Cell*. 24:9–12.
30. Strauss R, et al. (2011) Analysis of epithelial and mesenchymal markers in ovarian cancer reveals phenotypic heterogeneity and plasticity. *PLoS One*. 6:e16186.
31. Jiang P, Enomoto A, Takahashi M. (2009) Cell biology of the movement of breast cancer cells: intracellular signalling and the actin cytoskeleton. *Cancer Lett*. 284:122–30.
32. Kato K, et al. (2010) Endometrial cancer side-population cells show prominent migration and have a potential to differentiate into the mesenchymal cell lineage. *Am. J. Pathol.* 176:381–92.
33. Wang YH, et al. (2009) A side population of cells from a human pancreatic carcinoma cell line harbors cancer stem cell characteristics. *Neoplasma*. 56:371–8.
34. Bleau AM, et al. (2009) PTEN/PI3K/Akt pathway regulates the side population phenotype and ABCG2 activity in glioma tumor stem-like cells. *Cell Stem Cell*. 4:226–35.
35. Harris MA, et al. (2008) Cancer stem cells are enriched in the side population cells in a mouse model of glioma. *Cancer Res*. 68:10051–9.
36. Wu C, et al. (2007) Side population cells isolated from mesenchymal neoplasms have tumor initiating potential. *Cancer Res*. 67:8216–22.
37. Stiff PJ, et al. (2004) Randomized Phase II trial of two high-dose chemotherapy regimens with stem cell transplantation for the treatment of advanced ovarian cancer in first remission or chemosensitive relapse: a Southwest Oncology Group study. *Gynecol. Oncol.* 94:98–106.
38. Vuoriluoto K, et al. (2011) Vimentin regulates EMT induction by Slug and oncogenic H-Ras and migration by governing Axl expression in breast cancer. *Oncogene*. 30:1436–48.
39. Padua D, et al. (2008) TGF β primes breast tumors for lung metastasis seeding through angiopoietin-like 4. *Cell*. 133:66–77.
40. Horiguchi K, et al. (2009) Role of Ras signaling in the induction of snail by transforming growth factor- β . *J. Biol. Chem.* 284:245–53.
41. Ehata S, et al. (2011) Transforming growth factor- β decreases the cancer-initiating cell population within diffuse-type gastric carcinoma cells. *Oncogene*. 30:1693–705.
42. Hotz B, et al. (2007) Epithelial to mesenchymal transition: expression of the regulators snail, slug, and twist in pancreatic cancer. *Clin. Cancer Res*. 13:4769–76.
43. Hay ED. (2005) The mesenchymal cell, its role in the embryo, and the remarkable signaling mechanisms that create it. *Dev. Dyn.* 233:706–20.
44. Singh A, Settleman J. (2010) EMT, cancer stem cells and drug resistance: an emerging axis of evil in the war on cancer. *Oncogene*. 29:4741–51.
45. Morel AP, et al. (2008) Generation of breast cancer stem cells through epithelial-mesenchymal transition. *PLoS One*. 3:e2888.
46. Karst AM, Drapkin R. (2010) Ovarian cancer pathogenesis: a model in evolution. *J. Oncol.* 2010:932371.
47. Dyllal S, Gayther SA, Dafou D. (2010) Cancer stem cells and epithelial ovarian cancer. *J. Oncol.* 2010:105269.
48. Baba T, et al. (2009) Epigenetic regulation of CD133 and tumorigenicity of CD133+ ovarian cancer cells. *Oncogene*. 28:209–18.
49. Curley MD, et al. (2009) CD133 expression defines a tumor initiating cell population in primary human ovarian cancer. *Stem Cells*. 27:2875–83.
50. Zhang S, et al. (2008) Identification and characterization of ovarian cancer-initiating cells from primary human tumors. *Cancer Res*. 68:4311–20.
51. Wei X, et al. (2010) Mullerian inhibiting substance preferentially inhibits stem/progenitors in human ovarian cancer cell lines compared with chemotherapeutics. *Proc. Natl. Acad. Sci. U. S. A.* 107:18874–9.
52. Peters R, et al. (2010) Efficient generation of multipotent mesenchymal stem cells from umbilical cord blood in stroma-free liquid culture. *PLoS One*. 5:e15689.
53. Pozzi S, et al. (2006) Donor multipotent mesenchymal stromal cells may engraft in pediatric patients given either cord blood or bone marrow transplantation. *Exp. Hematol.* 34:934–42.
54. Veatch AL, Carson LF, Ramakrishnan S. (1994) Differential expression of the cell-cell adhesion molecule E-cadherin in ascites and solid human ovarian tumor cells. *Int. J. Cancer*. 58:393–9.
55. Katz E, Skorecki K, Tzukerman M. (2009) Niche-dependent tumorigenic capacity of malignant ovarian ascites-derived cancer cell subpopulations. *Clin. Cancer Res*. 15:70–80.
56. Bapat SA, Mali AM, Koppikar CB, Kurrey NK. (2005) Stem and progenitor-like cells contribute to the aggressive behavior of human epithelial ovarian cancer. *Cancer Res*. 65:3025–9.